

A.I. FEOKTISTOV, V.T. KUPRYASHKIN, L.P. SIDORENKO, N.F. KOLOMIETS,  
A.V. KOVALENKO, V.A. LASHKO

Institute for Nuclear Research, Nat. Acad. of Sci. of Ukraine  
(47, Prosp. Nauky, Kyiv 03680, Ukraine; e-mail: kupryashkinvt@yahoo.com)

**LOW-ENERGY SPECTRUM OF ELECTRONS EMITTED  
AT IRRADIATION OF A TITANIUM TARGET  
WITH  $\beta$ -PARTICLES OF TRITIUM  
AND  $\alpha$ -PARTICLES OF  $^{238}\text{Pu}$**

PACS 79.20.HX

*The low-energy spectrum of electrons emitted while bombarding a titanium target with  $\beta$ -particles obtained from a tritium source has been studied using the ( $\beta e$ )-coincidence method. To reveal common features and distinctions of this process for different charged particles under the same experimental conditions, including the same target, similar measurements are carried out using  $\alpha$ -particles ejected in the decay of  $^{238}\text{Pu}$ . It is shown that the ionization of atoms in the target at its bombardment with charged particles can be represented in the both cases as a result of the shake-off process.*

*Keywords:* reflection, passing through, near zero electrons ( $e_0$ -electrons), shake-off effect, microchannel plates (MCP)

## 1. Introduction

The low-energy spectrum of electrons arising owing to the bombardment of a titanium target with tritium-emitted  $\beta$ -particles can be presented as a result of the shake-off effect. The latter is a quantum-mechanical transition of the system (atom) from the initial nonexcited state  $i$  to a final state  $f$  under the influence of a sudden perturbation  $\frac{e^2}{r}$  induced by the interaction between the charge of a  $\beta$ -particle that passes by with the velocity  $V_\beta$  and the charge of an atomic electron at the time moment of their closest approach. As the “suddenness” of the shake-off effect, we mean that the emergence or variation of a charge occurs within a short time interval  $\tau$ , much shorter than the period of atom transition from the initial  $i$ -th state into the final  $f$ -th one, so that  $\tau_\beta = \frac{r}{V_\beta} \ll 2\pi\omega_{fi}^{-1}$ , where  $\omega_{fi}$  is the transition frequency.

The shake-off effect can be observed in the case where a sudden excitation arises spontaneously in a system at rest, e.g., at the  $\beta$ -decay, as well as when a charged particle moves near the target, at the time moment of its closest approach to target's atoms, when the probability of the shake-off event becomes dependent on the particle velocity  $V_\beta$ . In the former case, a modification of the interaction Hamiltonian

looks like  $H_0 \rightarrow H_0 + \Delta H$ , and this case is called the shake-off of the “switched-on interaction type”. In the latter case, the Hamiltonian modification has the form  $H_0 \rightarrow H_0 + \Delta H \rightarrow H_0$ , and this case is called the shake-off of the “scattering interaction type” [1]. Within the shake-off period  $\tau_p$ , the wave function  $\psi_i^{(0)}(q)$  of initial state of Hamiltonian  $H_0$  has no time to change [2] at the place, where the electron interacting with the particle charge is located, and almost all electrons in the atom remain at their places, except for the interacting electron, which transits onto an empty atomic level or becomes emitted into vacuum, leaving the final state of atom,  $\psi_f^*(q)$ , with a vacancy in the shell from which it was “shaken off”.

By researching the angular distribution of electrons emitted from the target surface at its bombardment with  $\alpha$ -particles, we revealed a number of electron emission types depending on the electron origin [3]. In the “forward” or transmission geometry, an  $\alpha$ -particle, when leaving the target, induces the emission of electrons from the target surface. In this case, we have three types of electron emission. These are electrons with a near-zero energy ( $e_0$ -electrons), which are shaken off from the target surface into vacuum owing to their interaction with a suddenly arisen motionless charge of ionized atoms that are located near the surface, as in the case of radioactive decay, and  $e_0$ -electrons, which are shaken off directly at their interaction with the passing-by charged particle. The kinetic energy of  $e_0$ -electrons,  $E$ , does not exceeds a

few electronvolts, and their binding energy at the surface,  $E_n$ , is lower than 1 eV (see the relevant discussion below). The angular distribution of  $e_0$ -electrons is directed strongly forward, along the normal to the surface.

Two other types of electron emission – in this case, we deal with fast  $e_f$ -electrons – are connected with the excitation of atoms at the time moment, when a charged particle passes by. If those atoms are in the target bulk, the shake-off stimulates an electron to transit onto an empty atomic level and a vacancy to emerge at the place, where the electron was located earlier. After the vacancy has been filled, the processes of Auger recombination take place, the result of which consists in that the fast  $e_f^A$ -electrons, which are engaged into those processes, can migrate toward the surface and escape into vacuum. They can be regarded as witnesses of the shake-off effect in the target. Their angular distribution should be isotropic, and we observed that in work [3].

At last, if a charged particle, when leaving the target, invokes a shake-off effect for electrons in the atoms located at the surface, the fast  $e_f^i$ -electrons are emitted into vacuum, which is accompanied by the emergence of vacancies in atoms at the places of electron escape. Since the  $e_f^i$ -electrons immediately penetrate into vacuum, their energy spectrum is not distorted, and it can be compared with the spectrum obtained theoretically in the framework of the shake-off effect model. (In this work, the spectra of  $e_f^i$ -electrons with energies below 400 eV will be considered. At higher energies, some spectral distortions may appear, e.g., due to the “tails” induced by convoy electrons.) The distribution of  $e_f^i$ -electrons over the angles of their emission from the target is close to the cosine one,  $\cos \theta$ , where  $\theta$  is the angle between the direction of  $e_f^i$ -electron emission and the normal to the surface at the surface point, where the charged particle escapes into vacuum [3].

In the reflection geometry, i.e. while registering the electrons emitted from the surface at the time moment when a charged particle is penetrating into the target, we observe  $e_0$ -electrons emitted mainly along the normal to the surface and, as it was in the case of the transmission measurements, the isotropic distribution of fast  $e_f^A$ -electrons. Hence, in both the “transmission” and “reflection” measurements, we see near-zero  $e_0$ -electrons and Auger  $e_f^A$ -electrons, whereas  $e_f^i$ -electrons are observed only in the transmission geometry. Since the  $e_f^A$ -electrons emitted from the target surface get directly into vacuum, this circumstance

enables a comparison of measured low-energy spectra of electrons with theoretical ones to be made, as was done by us, while studying the passage of  $\alpha$ -particles through Al, Cu, and Au targets [4–6]. The results of those researches demonstrated the adequacy of regarding the ionization of an atom by a passing-by particle as one of the shake-off effect manifestations.

In this work, we continued those researches. Now, as charged particles, we used  $\beta$ -particles with low energies emitted by decaying tritium atoms. As a target, we choose titanium. For the sake of comparison between the common and different features in the influence of  $\alpha$ - and  $\beta$ -particles on the shake-off process, we also carried out measurements for  $\alpha$ -particles emitted by  $^{238}\text{Pu}$  atoms under the same experimental conditions and with the same target, as in the experiment with the tritium decay. In addition, since tritium plays an important role in science and engineering, the obtained results may turn out useful in those domains.

## 2. Relations for Physical Quantities Describing the Shake-off Effect

The basic formula that describes the probability for an  $e_f^i$ -electron at the surface to escape into vacuum owing to its excitation by the interaction with a charged particle that suddenly passes by it looks like

$$dW(E) = \frac{c}{V_p} \left( \frac{Z_p e^2}{r} \right)^2 \left| \int \psi_f^* \psi_i^{(0)} dq \right|^2 \frac{b\sqrt{E}}{(E + E_n)^2} dE. \quad (1)$$

The first two multipliers determine the probability for the electron to be excited. The longer the excitation, the higher is the probability; of course, provided that the condition for the shake-off effect to take place, i.e.  $\tau_\beta \ll 2\pi\omega_{fi}^{-1}$ , is obeyed. The smallest probability of excitation takes place if the particle moves with the light velocity  $c$ . Although the dimensionality of the transferred excitation probability is defined as the squared energy, it is divided in formula (1) by the squared energy,  $(E + E_n)^2$ . The probability for the system to transit from the  $i$ -th state into the  $f$ -th one with a vacancy emerging instead of the emitted electron is determined by a square of matrix element composed of the coordinate parts of wave functions for the stationary states,  $\Psi(q, t) = \psi(q) \exp(-iE\frac{t}{\hbar})$ . At last, the last multiplier before  $dE$  corresponds to the differential distribution of electrons over their energies in the continuous spectrum after the shake-off event. The quantity  $b\sqrt{E} = \nu$  is the statistical distribution of the electron level density in the final state

of a continuous spectrum, where  $b = \frac{\sqrt{2m^3V_e}}{\pi^2\hbar^3}$ ,  $m$  is the electron mass,  $V_e = x^3$ , and  $x$  is the average distance between electrons capable of being shaken off into vacuum.

Hence, the first multipliers before the matrix element in Eq. (1) describe the first stage of the shake-off process. Namely, they determine the probability of excitation transfer, which depends on the velocity of charged particles. The other multipliers are related to the second stage of the shake-off process. In particular, they determine the probability for the system to transit from the initial state into the final one and the distribution of electrons over the energy in the continuous spectrum. The second stage does not depend on the kind of particles and their motion, although it is impossible alone, without the first stage.

While deriving expression (1), we used the formulas of perturbation theory in the first order of smallness for the time-dependent transitions at a sudden excitation of the system, which can be found in works [2–7], and appended them by the expression describing the process of electron shake-off into the continuous spectrum and the factor  $c/v_p$  that makes allowance for the charge motion at the time moment of excitation transfer [8]. The excitation is totally transferred to the shaken-off electron, and the system remains with a vacancy in the shell, from which the electron was shaken off. Then, for  $e_f^i$ -electrons at the surface, we have

$$\left(\frac{Z_p e^2}{r_a}\right) = E + E_n. \quad (2)$$

Although the transition probability of the system from the initial  $i$ -th state into a final  $f$ -th one does not depend on the excitation energy, the condition  $r < r_{\max}$ , where  $r_{\max} = \frac{Z_p e^2}{E_n}$  for  $e_f^i$ -electrons, must be satisfied, nevertheless. From the uncertainty relation, it follows that, at the time moment when the excitation is transferred from the charged particle to an electron in the atom, the uncertainty in the transferred energy  $\Delta E = \frac{\hbar}{\tau}$  is several times larger than the very magnitude of this excitation,  $E = \hbar\omega_{fi}$ , so that the main requirement of suddenness can be rewritten in the form  $\frac{\Delta E}{E} = \frac{\omega^{-1}}{\tau} \gg 1$ . At the time moment of perturbation, the energy transferred to electrons becomes uncertain. Therefore, the perturbation magnitude can be determined only after the energy of emitted electron has been measured, and the calculation by formula (2) has been carried out. Formula (2) can also be applied to find the distance  $r$ , at which the particle is passed by the shaken-off electron.

In the case of the charged particle passage through the target surface, the yield of  $e_f^i$ -electrons,  $\Upsilon(E)$ , in the energy interval from 0 to  $E$  is determined by the formula

$$\begin{aligned} \Upsilon(E) &= \pi \frac{c}{v_p} \left(\frac{Z_p e^2}{x}\right)^2 \left| \int \psi_f^* \psi_i^{(0)} dq \right|^2 b \int_0^E \frac{\sqrt{E} dE}{(E + E_n)^2} = \\ &= B \int_0^E \frac{\sqrt{E} dE}{(E + E_n)^2} = BF(E), \end{aligned} \quad (3)$$

$$F(E) = \int_0^E \frac{\sqrt{E} dE}{(E + E_n)^2} = \frac{1}{\sqrt{E_n}} \operatorname{arctg} \sqrt{\frac{E}{E_n}} - \frac{\sqrt{E}}{E + E_n},$$

$$F(0) = 0. \quad (4)$$

Formula (3) follows from formula (1) if one takes into account that the charged particle that crosses the target surface can interact with electrons of atoms that are located at the surface. If the intersection point of the charged particle path with the surface is considered as a circle center, then every electron within the ring  $\pi r_{\max}^2 - \pi r^2$ , when interacting with the charged particle, obtains the excitation energy necessary for it to be shaken off into vacuum with an energy from 0 to  $E$ , depending on its location. At  $r > r_{\max}$ , no shake-off event can take place because of the violation of the energy conservation law. At the same time, in the circle with the radius less than  $r$ , i.e. at the energy higher than  $E$ , the shake-off effect can also be not considered, because there are no such levels in the final state of the continuous spectrum in the interval from 0 to  $E$ . The number of  $e_f^i$ -electrons located in the ring from  $r$  to  $r + dr$  that can be shaken off into vacuum is determined by the expression  $|\pi r^2 - \pi r_{\max}^2|/x^2$ , where  $x^2$  is the surface area per one electron that can be shaken off into vacuum. At different points within the ring, electrons obtain different perturbation energies. However, owing to the sudden character of the perturbation and the uncertainty relation, the transferred perturbation becomes larger than the perturbation itself, and all electrons become indistinguishable with respect to the energy. The dependence of the shake-off probability on the electron energy is governed by the second stage of the process. The expression for the ring area by means of the absolute value is associated with a necessity – just in that order! – to put it in agreement with the integration limits over the energy from 0 to  $E$  in the formula for  $F(E)$ . Moreover, in what follows, the quantity  $\pi r_{\max}^2$

is multiplied by  $F(0) = 0$  and excluded from the further consideration. Therefore, the first stage of the shake-off process is responsible for the coefficient

$$\frac{c}{v_p} \frac{\pi r^2}{x^2} \left( \frac{ze^2}{r} \right)^2 = \pi \frac{c}{v_p} \left( \frac{z_p e^2}{x} \right)^2.$$

If the shake-off of an electron does not take place, the charged particle recovers the perturbation energy from the electron, and this scenario is similar to the procedure of insertion and removal of a probe charge.

### 3. Experimental Part

The low-energy spectrum of ionization electrons, which arose after a tritium-emitted  $\beta$ -particle had passed through the titanium target, was studied with the use of the method of  $(\beta e)$ -coincidences in time and applying the decelerating voltage  $U$  (the retarding potential) in the electron registration channel. The dependence of the rate of time-coincidence counting on the decelerating voltage applied to the target was measured. The temporal spectra of coincidences were registered on a multichannel analyzer ORTEC-NORLAND.

The measurements were carried out in two experimental geometries depicted in Fig. 1. In the “transmission” setup (Fig. 1,*a*), tritium source *S* together with collimator *K* was arranged near target *T* as is exhibited in the figure. A self-supporting titanium film  $0.4 \mu\text{m}$  in thickness served as a target. It was oriented at an angle of  $45^\circ$  with respect to the  $\beta$ -particle beam, so that the total path passed by  $\beta$ -particles in the film amounted to  $0.57 \mu\text{m}$ . After  $\beta$ -particles had passed through the target, they arrived at a microchannel plate (MCP) detector,  $\text{MCP}_1$ , arranged at a distance of 6 cm and were registered by it. The latter consisted of two microchannel plates combined with each other in the form of a chevron. At the same time,  $e_{0-}$ ,  $e_f^A$ , and  $e_f^i$ -electrons emitted from the target when a  $\beta$ -particle passed through it were registered by another detector,  $\text{MCP}_2$ . Detector  $\text{MCP}_2$  was mounted immovably in the vacuum chamber, whereas all other constructional elements— $\text{MCP}_1$ , *S*, *K*, and *T*—were mounted on shaft *O* (the rotation axis). This arrangement enabled the angular distribution of electrons arriving at  $\text{MCP}_2$  at their coincidence in time with  $\beta$ -particles to be measured. The target, the collimator, and the source had the identical potential  $U$ , which could be changed in the course of measurements. The chamber vacuum pressure was maintained at a level of  $5 \times 10^{-6}$  mm Hg.

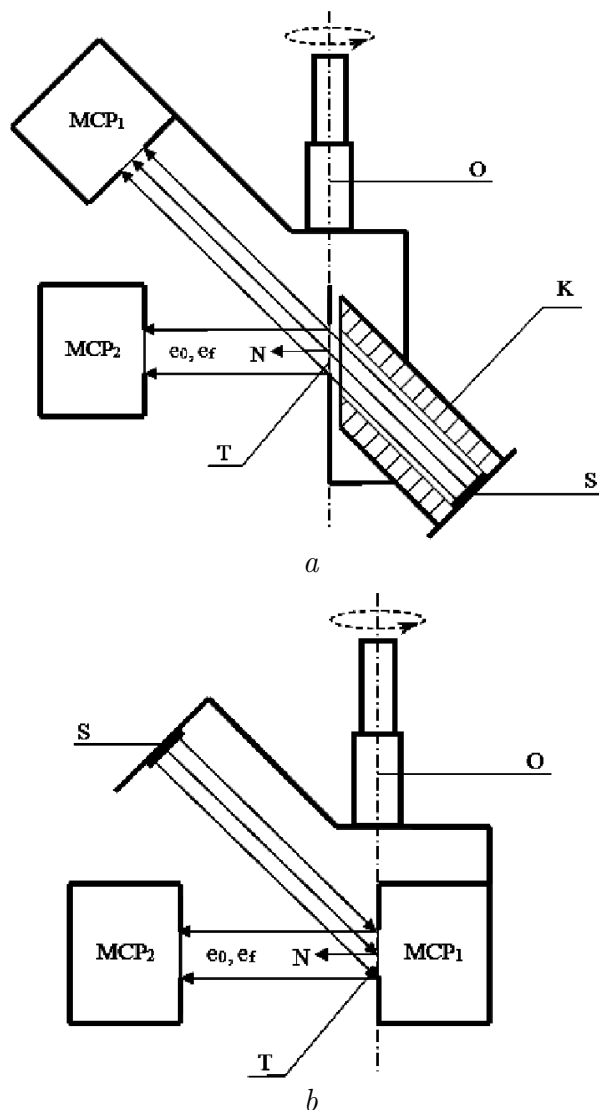


**Fig. 1.** (a) Transmission and (b) reflection experimental setups: source *S*, target *T*, detectors  $\text{MCP}_1$  and  $\text{MCP}_2$ , collimator *K*, and rotation axis *O*

In the “reflection” experimental geometry (Fig. 1,*b*), a  $\beta$ -particle detector  $\text{MCP}_1$  was arranged immediately behind the target, whereas source *S* (without the collimator) was removed onto the previous place of  $\text{MCP}_1$  detector. In this fashion,  $\text{MCP}_2$  detector registered  $e_{0-}$  and  $e_f$ -electrons emitted when an  $\beta$ -particle penetrated into the target, to which the potential  $U$  was applied. The same target surface was studied in both setups.

As a radioactive source, we used a spot of tritium 7.5 mm in diameter inserted into a titanium substrate 35 mm in diameter. The average energy of tritium-

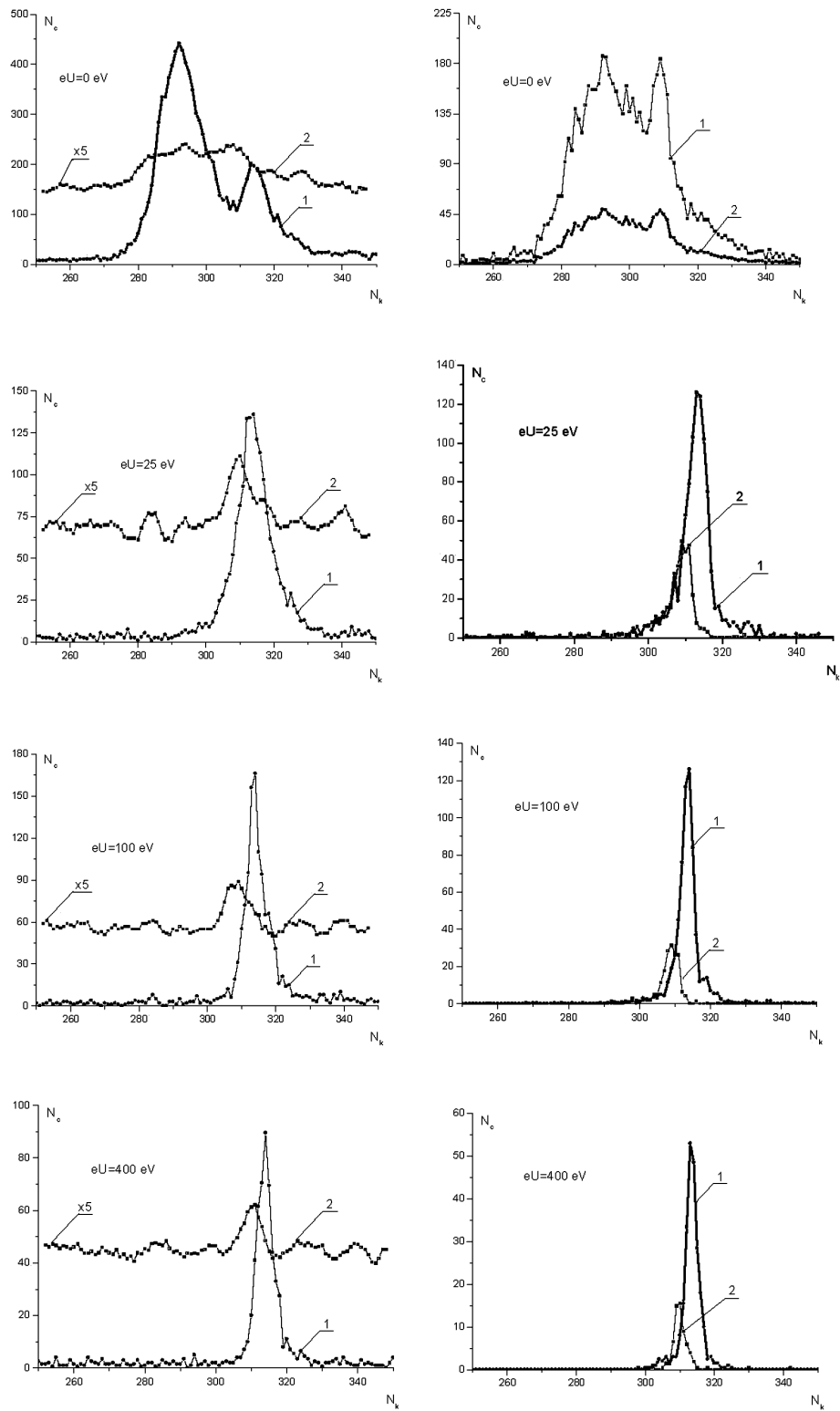


**Fig. 2.** Spectra of  $(\beta e)$ - (left panels) and  $(\alpha e)$ -coincidences (right panels) in time measured at various retarding potentials at the target in “transmission” (curves 1) and “reflection” (curves 2) experiments.  $N_k$  is the number of analyzer channel

emitted  $\beta$ -particles amounted to  $5.69 \pm 0.02$  keV with an energy maximum of 18 keV, and the source activity was  $5 \times 10^7$  Bq. To simplify calculations, we neglected a small number of  $\beta$ -particles emitted with energies from 16 to 18 keV and regarded the electron distribution in the hard spectral range as a hypotenuse of the rectangular triangle. In the transmission geometry, owing to the absorption of  $\beta$ -particles, detector MCP<sub>1</sub> registered only electrons with the initial energy higher than 8.4 keV, which corresponded to the mean free path of electrons in the target depth. The average velocity of  $\beta$ -particles leaving the target was  $V_\beta = 3.8 \times 10^9$  cm/s, and their average energy was  $E = 3.7$  keV, which will be discussed below. In the reflection geometry, the average energy of those  $\beta$ -particles entering the target, which could pass through it and be registered by detector MCP<sub>1</sub>, amounted to 11 keV, which corresponded to their average velocity  $V_\beta = 6.3 \times 10^9$  cm/s.

At measurements with  $\alpha$ -particles, the tritium source was simply substituted by a  $^{238}\text{Pu}$  source from the OSAI collection of standard spectrometric alpha-particle sources – a reference source for spectrometry with the energy of  $\alpha$ -particles  $E = 5.5$  MeV. For  $\alpha$ -particles, the target was rather thin; therefore, their energies at entering the target and leaving it were practically identical, so that their velocity  $V_\alpha = 1.6 \times 10^9$  cm/s was adopted in both cases.

In Fig. 2, the fragments of the time coincidence spectra measured in the transmission (curves 1) and reflection (curves 2) geometries at various values of retarding potential  $U$  are depicted. The left and right panels illustrate the spectra obtained for the passage of  $\beta$ - and  $\alpha$ -particles, respectively, through the target. One can see from the figure that, if the retarding potential  $U = 0$  V, the spectra demonstrate two peaks: from  $e_0$ - (the left peak) and  $e_f$ -electrons (the right one). As the potential grows, the intensity of  $e_0$ -peak rapidly falls down, and it almost completely disappears at the energy  $eU = 24$  eV. We have studied the properties of  $e_0$ -electrons thoroughly enough in works [9–12]; therefore, we dwell now on them only shortly. For the illustrative purpose, in Fig. 3, the dependence  $N(E = eU)$  obtained while measuring the coincidences of  $e_0$ -electrons and tritium-emitted  $\beta$ -particles in the transmission geometry and  $U$  varying from +24 to  $-10$  eV is shown by curve 1. The increase in the number of coincidences  $N_{\beta e}$  at  $U < 0$  is associated with an increase of the space angle at the electron registration by detector MCP<sub>2</sub> owing to an increase of the extraction voltage applied be-

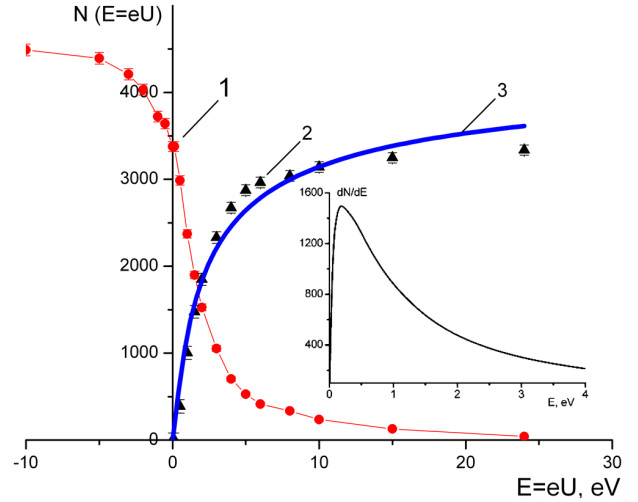


**Fig. 3.** Spectra of electrons shaken off owing to their interaction with tritium-emitted  $\beta$ -particles obtained in “transmission” measurements: (1) delay curve (the integrated spectrum of electrons in the energy interval from  $E_{\max}$  to  $E = eU$ ), (2,  $\blacktriangle$ ) integrated distribution of  $e_0$ -electrons in the energy interval from 0 to  $E$ , and (3) energy distribution of electrons calculated by formula (4) for the shake-off effect with  $E_n = 0.6$  eV. The inset demonstrates the differential distribution of  $e_0$ -electrons calculated for this binding energy by formula (3)

tween the target and the detector. We shall consider the energy distribution of  $e_0$ -electrons only in the interval from 0 to  $E$  and in terms of the difference  $N_\Delta(E) = N(0) - N(E) = AF(E)$  between the number of ( $\beta e_0$ )-coincidences in the intervals from  $E_{\max}$  to 0, i.e.  $N(0)$ , and from  $E_{\max}$  to  $E$ , i.e.  $N(E)$ , where  $F(E)$  is the theoretical distribution of shaken off  $e_0$ -electrons calculated by formula (4). As one can see from Fig. 3, the experimental distribution  $N_\Delta(E)$  agrees well with the theoretical one (curve 3). Fitting was carried out using the least-squares method. The calculated binding energy of electrons at the surface of a Ti target was found to equal  $E_n = 0.6 \pm 0.1$  eV, and  $A = 2274 \pm 255$ .

Now, let us return to studying the time spectra of coincidences for fast  $e_f$ -electrons. Some of their fragments are shown in Fig. 2. Owing to a considerable number of random coincidences obtained in the “reflection” spectra owing to tritium-emitted  $\beta$ -particles, a five-point smoothing was carried out. In addition, at “transmission” measurements, both  $\alpha$ - and  $\beta$ -particles passed a shorter distance within the time interval between the time moment of flying out of the target and the moment of their registration; therefore, their peaks in the “transmission” time spectra became shifted toward smaller registration times with respect

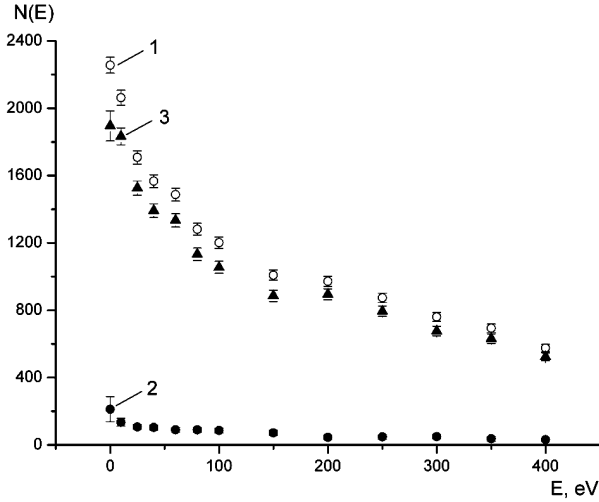


**Fig. 4.** Energy dependences of the number of coincidences between  $\beta$ -particles and fast  $e_f$ -electrons: (1) in the “transmission” geometry, (2) in the “reflection” geometry, and (3) for  $e_f^i$ -electrons shaken off into vacuum

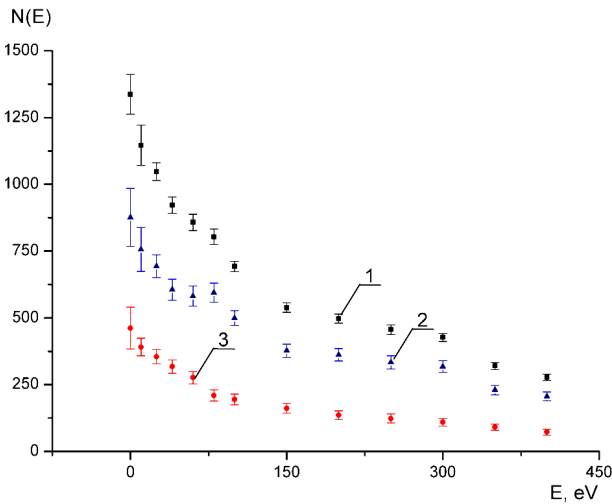


**Fig. 5.** The same as in Fig. 4, but for coincidences between  $\alpha$ -particles and fast  $e_f$ -electrons

to their counterparts in the “reflection” time spectra. For the same reason, in “reflection” measurements, the value of  $N_\beta$  was five and the value of  $N_\alpha$  two times as large as the corresponding values obtained in the transmission geometry for the same measurement period. All spectra were normalized to the corresponding counting rate, namely,  $n_\beta = 3.6 \times 10^6$   $\beta$ -particles per hour or  $n_\alpha = 1.8 \times 10^5$   $\alpha$ -particles per hour. (Note, however, that the “reflection” spectra for  $\beta$ -particles in Fig. 2 are scaled up by a factor of five for the illustrative reason.)

In this work, we measured the time spectra of coincidences in the interval of decelerating voltage from 0 to 400 V. In all, we measured 13 points with an exposition of 1 h each.

#### 4. Experimental Results and Their Discussion

Now, let us proceed to the discussion of the properties of fast  $e_f$ -electrons. In Fig. 4, distribution 1 demonstrates the number of  $(\beta e_f)$ -coincidences calculated as a sum of  $e_f^A$ - and  $e_f^i$ -electrons measured in the transmission geometry as a function of the energy,  $N_{\beta 1}(eU)$ . Distribution 2 shows the same dependence for the number of  $(\beta e_f^A)$ -coincidences measured in the reflection geometry,  $N_{\beta 2}(eU)$ . At last, distribution 3 corresponds to the number of registered  $e_f^i$ -electrons, which is determined as the difference  $N_{\beta 3}(eU) = N_{\beta 1}(eU) - 1.7N_{\beta 2}(eU)$ . A coefficient of 1.7 arose because the probability of a shake-off event at the exit from the target, where  $v_\beta = 3.8 \times 10^9$  cm/s, is 1.7 times higher than that at the entrance, where  $v_\beta = 6.3 \times 10^9$  cm/s.

Figure 5 exhibits the same dependences as in Fig. 4, but for  $\alpha$ -particles passing through the target. The distribution for  $e_f^i$ -electrons was determined as the difference  $N_{\alpha 3}(eU) = N_{\alpha 1}(eU) - N_{\alpha 2}(eU)$ . Since the titanium target was thin for  $\alpha$ -particles, the number of  $e_f^A$ -electrons was the same at the entrance to and the exit from the target.

On the basis of formula (1), we can compare the distributions  $N_{\beta 3}(eU)$  and  $N_{\alpha 3}(eU)$ . For instance,  $\frac{N_{\alpha 3}(0) \times n_\beta}{N_{\beta 3}(0) \times n_\alpha} = \frac{876 \times 20}{1832} = 9.57$ . At the same time, according to formula (1),  $\frac{z_\alpha^2 \times v_\beta}{1 \times v_\alpha} = \frac{4 \times v_\beta}{1 \times 1.6}$ . Whence, the velocity of  $\alpha$ -particle at the exit  $v_\beta = 3.8 \times 10^9$  cm/s. This value of  $v_\beta$  for  $\beta$ -particles was used by us earlier in the calculations for the transmission mode. The presented ratio differs insignificantly for other points ( $eU$ ) and amounts to 8.8 on the average, which means a similarity between the shake-off curves for  $\alpha$ - and  $\beta$ -particles.

We can also compare the distributions for  $e_f^A$ -electrons. In particular, for electrons shaken off onto excited atomic levels in the target in the cases of passing  $\alpha$ - and  $\beta$ -particles,  $\frac{N_{\alpha 2}(0)}{N_{\beta 2}(0)} = \frac{467 \times 20 \times 2}{215 \times 5} = 17.4 \times 10^9$  cm/s, whereas, according to formula (1),  $\frac{z_\alpha^2 \times v_\beta}{1 \times v_\alpha} = \frac{4 \times 6.3}{1 \times 1.6} = 15.8 \times 10^9$  cm/s. This means that the both distributions of electrons in the reflection geometry are similar. The multiplier 2/5 arises, because, in the reflection geometry, the number of  $\beta$ -particles counted during the measurement

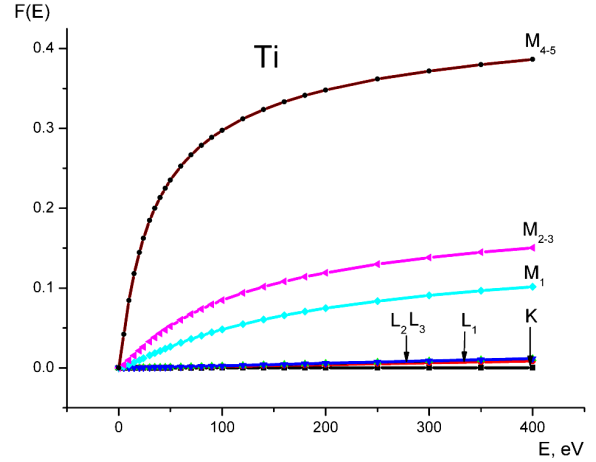
time,  $n_\beta$ , is five times larger than that in the reflection geometry, and the number of  $\alpha$ -particles,  $n_\alpha$ , is twice as large. This is connected with the fact that, owing to the scattering of  $\alpha$ - and  $\beta$ -particles at their passage through the target, half as many  $\alpha$ -particles and one-fifth as many  $\beta$ -particles arrive at detector MCP<sub>1</sub> in the transmission geometry in comparison with the corresponding values for the reflection geometry, in which detector MCP<sub>1</sub> is located immediately behind the target so that those losses are absent.

The measurements of the angular distribution of emitted  $e_f$ -electrons when the target was irradiated with  $\beta$ -particles in the transmission mode and at a number of energies in the integrated spectra  $N_{\beta 1}(eU)$  showed that, for every of them, the angular distribution is directed forward, and its shape is close to the cosine. The angular distribution was also measured at the excitation of target atoms with  $\alpha$ -particles, but only in the case  $eU = 0$  eV. Its comparison with the analogous distribution obtained at  $\beta$ -excitation revealed a certain similarity between them. Analogous measurements for  $e_f^A$ -electrons in the reflection mode were not carried out owing to a large number of random coincidences between  $\beta$ -particles and  $e_f^A$ -electrons. Nevertheless, it was found in work [3] that, in the case of  $\alpha$ -particle irradiation, all flying out  $e_f^A$ -electrons had an isotropic angular distribution in the reflection geometry.

The integrated spectrum of ionization  $e_f^i$ -electrons in the energy interval from 0 to  $E$  can be obtained after carrying out the transformation that corresponds to the change of integration limits,  $\int_0^E = \int_0^{E_{\max}} - \int_E^{E_{\max}}$ , i.e.  $N_{\beta 4}(E) = N_{\beta 3}(0) - N_{\beta 3}(E)$ , and comparing it with the theoretical distribution  $N_{\beta 4}(E) = \sum_l A_{\beta l} F_l(E)$ , where the subscript  $l$  denotes different atomic shells that participate in the shake-off effect, and the multiplier  $A_{\beta l}$ , which does not depend on the energy distribution of  $e_f^i$ -electrons, is determined as follows:

$$A_{\beta l} = \eta \pi \frac{c}{V_\beta} \left( \frac{z_\beta e^2}{x_l} \right)^2 \left| \int \psi_f^* \psi_i^{(0)} dq \right|_l^2 b n_\beta,$$

Here, the quantity  $\eta$  depends on experimental conditions and is expressed as a product of the electron registration efficiency  $\varepsilon$  and the fraction of electrons collected by detector MCP<sub>2</sub>,  $\delta_{\text{eff}}$ ; and  $n_l$  is the number of electrons in the  $l$ -th subshell. In the case of passing  $\alpha$ -particles, all the subscripts  $\beta$  in this formula should be substituted by the subscripts  $\alpha$ .



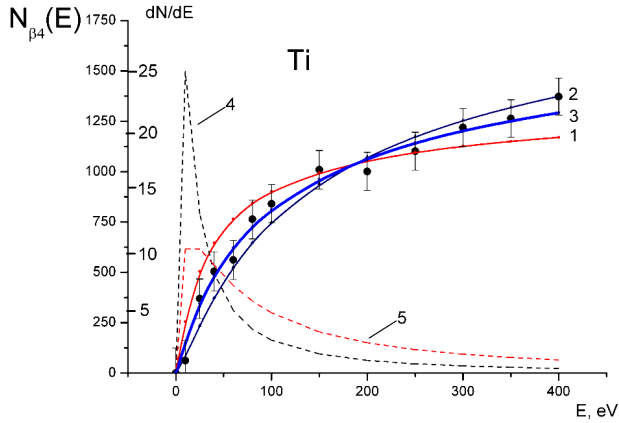
**Fig. 6.** Function  $F(E)$  describing the integrated energy distribution of  $e_f$ -electrons (see formula (4)) shaken off from various subshells of a Ti atom

Figure 6 illustrates the results of calculations by formula (4) for the integrated energy distribution of  $e_f^i$ -electrons in various subshells of a titanium atom. Below, we shall demonstrate that only the distributions calculated for electrons that are shaken off from M-subshells are comparable with experimental ones, whereas the K- and L-shells weakly affect the shake-off phenomenon for  $e_f^i$ -electrons in this energy interval.

In Fig. 7, the experimental and theoretical energy distributions are compared. The latter was fitted for  $e_f^i$ -electrons shaken-off by tritium-emitted  $\beta$ -particles, using the least-squares method. The experimental values are shown by circles, with the corresponding statistical errors being indicated by bars. Curve 1 was obtained in the case where  $e_f^i$ -electrons were shaken off only from the  $M_{4,5}$ -subshells of titanium atom, and curve 2 when only from the  $M_{1,2,3}$ -subshells. Bold curve 3 illustrates the results of calculations for the case of the combination  $N_{\beta 4}(E) = N_\beta(E) = x A_{M_{4,5}} F_{M_{4,5}}(E) + (1-x) A_{M_{1,2,3}} F_{M_{1,2,3}}(E)$  with  $x = 0.4$ .

A similar analysis was carried out for electrons shaken off from the Ti target bombarded with  $\alpha$ -particles emitted by decaying  $^{238}\text{Pu}$ . The corresponding results are shown in Fig. 8. According to them, the energy distribution of ionization  $e_f^i$ -electrons in the cases of irradiation with both tritium  $\beta$ -particles and  $^{238}\text{Pu}$   $\alpha$ -particles can be described as such that is mainly formed by the electron shake-off from the M shells (40% from the  $M_{4,5}$  subshells + 60% from the  $M_{1,2,3}$  subshells) of Ti atoms. Taking into account that the ionization potential for Ti equals 6.8 eV, the





**Fig. 7.** Comparisons between experimental and calculated distributions of  $e_f$ -electrons shaken off by tritium-emitted  $\beta$ -particles from the  $M_{4,5}$  (1) and  $M_{1,2,3}$  (2) subshells of a Ti atom, and (3) if their mixture is taken into account. Dotted curved show the differential energy distributions of  $e_f$ -electrons for the  $M_{4,5}$  (4) and  $M_{1,2,3}$  (5) subshells

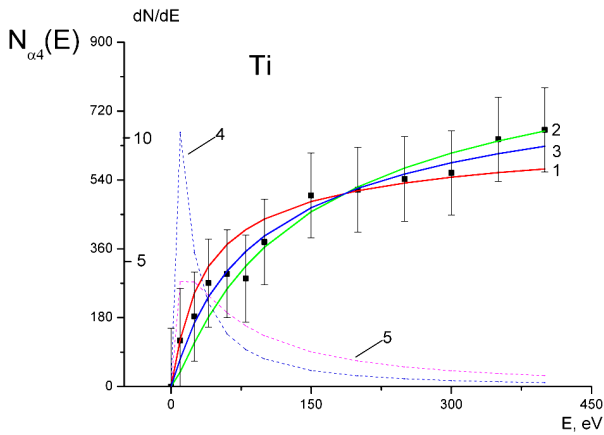


**Fig. 8.** The same as in Fig. 7, but for  $e_f$ -electrons shaken off by  $\alpha$ -particles from decaying  $^{238}\text{Pu}$

binding energies  $E_n$  were taken to equal 10.5 eV for the  $M_{4,5}$  subshells, and, for the  $M_{1,2,3}$  subshells, to their average value of 47.8 eV. The dotted curves in Figs. 7 and 8 demonstrate the calculated differential spectra of  $e_f$ -electrons obtained by formula (3) for those components of the curve  $N_{\beta 4}$ .

Hence, the contribution of each of two electrons in the  $M_{4,5}$  subshells of a Ti atom is responsible for 20% of the total shake-off probability, and each of eight electrons in the  $M_{1,2,3}$  subshells gives a contribution of 7.5%. The ratios between the squared matrix elements for the transition from those  $i$ -th states into the final  $f$ -th state must correspond to those values. Since the quantity  $\eta$  is uncertain (we took it

equal to  $\eta = 5 \times 10^{-3}$ ), the transition matrix elements can be only estimated:  $|M_{fi}|_{M_{4,5}} = 3.6 \times 10^{-2}$  and  $|M_{fi}|_{M_{1,2,3}} = 4.1 \times 10^{-2}$ .

## 5. Conclusions

Our experimental researches of the energy distribution for  $e_f^i$ -electrons emitted from a titanium target when the latter is bombarded with tritium-emitted  $\beta$ -particles showed its good agreement with that calculated by formula (1). This allows a conclusion to be drawn concerning the adequacy of the description of the atomic ionization by a passing-by charged particle as a quantum-mechanical transition in the system from the initial state into a final one under the action of a sudden perturbation, which is accompanied by the emission of electron with an energy in the continuous part of the spectrum and by the emergence of a vacancy in the atom instead of the emitted electron, i.e. as the shake-off effect. Such a conclusion was made by us earlier, while studying the ionization of various targets by passing-by  $\alpha$ -particles [4–6].

A comparison of shake-off properties was made for the cases of  $\alpha$ - and  $\beta$ -particles passing through a Ti target. For this purpose, the corresponding analogous measurements were carried out under the same experimental conditions. The resulting energy distributions of  $e_f^i$ -electrons turned out similar to each other, and the total probability of a shake-off event is proportional to  $(z_p e^2)^2 / v_p$ .

The process of electron shake-off can be imagined as having two stages [13]. At the first stage, the system is suddenly excited, and the experiment testifies to a difference between the probabilities of perturbation transfer in the cases of passing  $\alpha$ - and  $\beta$ -particles; it is determined by the first two multipliers,  $\pi \frac{c}{v_p} \left( \frac{z_p e^2}{r_a} \right)^2$ , in formula (1). At the second stage, the system transits from the initial  $i$ -th state into a final  $f$ -th one. The second stage is represented by the other terms in formula (1) and runs identically for various particles and independently of the first stage (although the very existence of the second stage is impossible without the existence of the first one). This conclusion was also confirmed by comparing the results of our measurements carried out in this work.

1. A.M. Dykhne and G.L. Yudin, *Usp. Fiz. Nauk* **125**, 377 (1978).
2. L.D. Landau and E.M. Lifshitz, *Quantum Mechanics. Non-Relativistic Theory* (Pergamon Press, New York, 1977).

3. V.T. Kupryashkin, L.P. Sidorenko, A.I. Feoktistov, and I.P. Shapovalova, *Izv. Akad. Nauk SSSR. Ser. Fiz.* **68**, 1208 (2004).
4. L.P. Sidorenko, V.T. Kupryashkin, O.I. Feoktistov, and E.P. Rovenskikh, *Ukr. Fiz. Zh.* **55**, 757 (2010).
5. V.T. Kupryashkin, L.P. Sidorenko, A.I. Feoktistov, and E.P. Rovenskikh, *Zh. Eksp. Teor. Fiz.* **139**, 679 (2011).
6. V.T. Kupryashkin, L.P. Sidorenko, A.I. Feoktistov, and E.P. Rovenskikh, *Ukr. Fiz. Zh.* **57**, 5 (2012).
7. A.S. Davydov, *Quantum Mechanics* (Pergamon Press, New York, 1976).
8. O.I. Feoktistov, *Ukr. Fiz. Zh.* **55**, 165 (2010).
9. O.I. Feoktistov, *Ukr. Fiz. Zh.* **53**, 1043 (2008).
10. V.T. Kupryashkin, L.P. Sidorenko, A.I. Feoktistov, and I.P. Shapovalova, *Izv. Akad. Nauk SSSR. Ser. Fiz.* **67**, 1446 (2003).
11. A.I. Feoktistov, A.A. Valchuk, V.T. Kupryashkin, L.P. Sidorenko, and I.P. Shapovalova, *Izv. Ross. Akad. Nauk. Ser. Fiz.* **72**, 281 (2008).
12. A.I. Feoktistov, A.A. Valchuk, V.T. Kupryashkin, L.P. Sidorenko, and I.P. Shapovalova, *Izv. Ross. Akad. Nauk. Ser. Fiz.* **72**, 285 (2008).
13. A.M. Dykhne and G.L. Yudin, *Usp. Fiz. Nauk* **121**, 157 (1977).

Received 28.03.12.

Translated from Ukrainian by O.I. Voitenko

*О.І. Феоктістов, В.Т. Купряшкін, Л.П. Сидоренко,  
М.Ф. Коломієць, О.В. Коваленко, В.А. Лашко*

НИЗЬКОЕНЕРГЕТИЧНІ СПЕКТРИ ЕЛЕКТРОНІВ,  
ЯКІ ВИНИКАЮТЬ ПРИ БОМБАРДУВАННІ  
ТИТАНОВОЇ МІШЕНІ  $\beta$ -ЧАСТИНКАМИ  
ТРИТІЮ ТА  $\alpha$ -ЧАСТИНКАМИ  $^{238}\text{Pu}$

Резюме

Методом часових ( $\beta e$ )-збігів досліджено низькоенергетичний спектр електронів, які виникають при бомбардуванні мішені титану  $\beta$ -частинками з розпаду тритію. Щоб порівняти спільні риси та відмінності у впливі різних заряджених частинок на цей процес, в тих же експериментальних умовах і з тою самою мішенню, аналогічні вимірювання було проведено з  $\alpha$ -частинками з розпаду  $^{238}\text{Pu}$ . Показано, що іонізацію атомів при бомбардуванні мішені зарядженими частинками можна представити як ефект струсу в обох випадках.